Eur. Phys. J. D **44**, 497–505 (2007)
DOI: 10.1140/epjd/e2007-00203-9

THE EUROPEAN PHYSICAL JOURNAL D

On the energy dependence of inelastic cross sections

A.K. Belyaev[a]

Department of Theoretical Physics, Herzen University, St. Petersburg 191186, Russia

Received 27 November 2006 / Received in final form 23 April 2007
Published online 20 June 2007 –

Abstract. The new accurate two-state quantum calculations of the inelastic cross sections in H + Li, Na collisions for energies from the thresholds and till 100 eV or 600 eV are performed, and the results are compared with the Landau-Zener model cross sections in both the diabatic and the adiabatic representations. It is found that the low-energy inelastic cross section is very sensitive to nonadiabatic coupling and, hence, the new NaH coupling is computed. The numerical solutions of the coupled channel equations are checked by independent calculations indicating that the quantum results are accurate. These checks are done by means of the analytic formula for a nonadiabatic transition probability derived within the perturbation approach. Both the Landau-Zener-like and the non-Landau-Zener-like behaviour of the excitation cross sections are found.

PACS. 34.10.+x General theories and models of atomic and molecular collisions and interactions – 34.50.Fa Electronic excitation and ionization of atoms 34.70.+e Charge transfer

1 Introduction

Heavy particle collision processes are of both fundamental and practical importance in determining the properties of non-equilibrium gases such as occur in planetary and stellar atmospheres, lasers, and weakly ionized plasmas [1,2]. In few cases the cross sections that are needed to calculate the excited level population and to interpret the spectral line data are known. In the great majority of cases, the required data are not available. Inelastic cross sections can be obtained from both experiments and numerical calculations. Experiments on inelastic low-energy (below 1 keV) atomic collisions are challenging, so atom-atom collisions have been investigated at low energies only for a small number of experimentally favorable cases. On the other hand, although numerical calculations offer no difficulties in principle [3,4], the number of theoretical papers dealing with atomic or ionic collisions with energies of a few eV is small, probably because of the lack of reliable quantum chemical data.

Inelastic atomic collisions are of importance for the line formation in non-local thermodynamic equilibrium models of stellar atmospheres [1,2,5,6]. The construction of photospheric models is highly tentative, because even the order of magnitude of the relevant cross sections is unknown [1,2]. Steenbock and Holweger [5] first pointed out the possible importance of inelastic collisions of metal atoms with hydrogen in metal-poor dwarfs. They estimated the collisional excitation rates for X + H by modifying a formula from Drawin [7] for H + H which is itself a modification of the classical Thomson formula for excitation by electrons (cf. [1]). In recent years some progress has been made for the H + Na, Li systems. Low-energy (between 10 eV and 600 eV) H + Na experimental data have been obtained [8] and the quantum dynamical calculations for H + Na [9] and H + Li (below 10 eV) [10] have been performed down to the energy thresholds. It was found that the modified Drawin formula overestimates the H + Na($3s$) → H + Na($3p$) and H + Li($2s$) → H + Li($2p$) collision rates by several orders of magnitude [9,10]. Nevertheless, estimates are required for transitions between all states which might affect the population, and the modified Drawin formula is still in use amongst the astrophysics community despite its overestimation of the collision rates.

The alternative to the modified Drawin formula is the Landau-Zener (LZ) model [11,12] (see also [13]). This model and its modifications are widely used in the atomic and molecular physics community. It has been shown [9,10] that the LZ model gives results much closer to the quantal ones than the modified Drawin formula. In the standard version [13], the LZ model is formulated as a two-state problem in the basis of diabatic states. There exist different modifications of the Landau-Zener model, e.g. the multichannel models [14–18], and other nonadiabatic models [19–22]. The model has been subjected to detailed analyses [23–25] as well. In practical applications the requirements of the LZ model are seldom fulfilled. Nevertheless the LZ model is the most widely used for estimates of nonadiabatic transition probabilities in its standard two-state version despite its limitation.

[a] e-mail: andrey.belyaev@ch.tum.de

It should be pointed out that in some phenomena the excitation cross sections in the energy threshold regions are of the main interest. For example, in cool star atmospheres the temperature range is 2000–8000 K, and hence the low energy collisions just above the threshold (0.2–1 eV) are most important in determining the collision rates for typical optical transitions [1,6]. It is known that in such the cases, where the cross sections are small, the standard version of the Landau-Zener model is not reliable any more, but it is still in use, which leads to the questions how large is a deviation of the LZ model cross sections from the quantal values, how accurate the quantal cross sections, and how sensitive they are to the quantum chemical data. Moreover, in practical applications the energy dependence of the cross section at low-energy collisions can deviate from the behaviour of the cross section at higher energies. The understanding of origins for such the deviation is of interest. For this reason in the present paper the quantal cross sections for the excitation processes in H + Li, Na collisions are recalculated within the two-state treatment and compared with the results of the standard Landau-Zener model. These collisional systems are similar. At low energies the nonadiabatic transitions between the $^1\Sigma^+$ molecular states dominate over transitions between other states [9,10]. The main interest is in transitions between the two lowest molecular states: $X\ ^1\Sigma^+$ and $A\ ^1\Sigma^+$. If the collision energy is high enough, more than one excited channels can be populated during the collisions, but at low collision energies the population of states other than Li($2p$) and Na($3p$) does not exceed a few per cents of the total population [9,10]. Thus the two-state approximation can be adopted with high accuracy.

In the present work an additional check of the quantal calculations is also performed by the independent approach; this is done within the perturbation theory. The derived approach allows one to understand the unusual behaviour of the H + Na($3s$) → H + Na($3p$) and H + Li($2s$) → H + Li($2p$) cross sections at low collision energies.

2 Brief theory outlook

2.1 Coupled channel equations

Inelastic transition probabilities and cross sections can be calculated by solving of coupled channel equations within the standard adiabatic approach, see, for example, [4,21]. To obtain the equations in the adiabatic representation one writes the total wave function Ψ for the system as a sum of terms $\Psi_{J\,M_J}$ characterized by the total angular momentum quantum numbers J and M_J ($M_J \geq 0$) and expands the $|\Psi_{J\,M_J}\rangle$ state in the basis of adiabatic electronic states $|j\rangle$. For the molecular Σ states this expansion is given by

$$|\Psi_{J\,M_J}\rangle = Y_{JM_J}(\Theta,\Phi)\sum_j \frac{F_j(R)}{R}\,|j\rangle, \qquad (1)$$

where $Y_{J\,M_J}$ are the spherical harmonics; Θ and Φ are the spherical coordinate angles of the vector $\mathbf{R}$ connecting the nuclei. In the framework of the standard adiabatic approach the Jacobi coordinates are used. The functions $F_j(R)$ describe the radial motion of the nuclei. Substituting the expansion (1) into the stationary Schrödinger equation $(H - E_{tot})\Psi_{J\,M_J} = 0$ [H being the total Hamiltonian, $E_{tot} = E + V_i(\infty)$ being the total energy, $V_j(R)$ being the adiabatic potential energy for the channel j, and E being the collision energy], one obtains a set of the coupled channel equations (CCE) in the adiabatic representation [4,9,10,26]

$$\left[-\frac{\hbar^2}{2M}\frac{d^2}{dR^2} + V_j(R) + \frac{\hbar^2}{2M}\frac{J(J+1)}{R^2} - E_{tot}\right]F_j(R) =$$

$$\frac{\hbar^2}{M}\sum_k \langle j|\frac{\partial}{\partial R}|k\rangle\,\frac{dF_k(R)}{dR} + \frac{\hbar^2}{2M}\sum_k \langle j|\frac{\partial^2}{\partial R^2}|k\rangle\,F_k(R). \qquad (2)$$

The adiabatic potentials $V_j(R)$ and single derivative nonadiabatic matrix elements can be calculated by quantum chemical programs. The double derivative couplings are not usually calculated explicitly, but may be estimated from the single derivative couplings [9]

$$\left\langle j\left|\frac{\partial^2}{\partial R^2}\right|k\right\rangle = \frac{d}{dR}\left\langle j\left|\frac{\partial}{\partial R}\right|k\right\rangle. \qquad (3)$$

The problem can be also solved in a diabatic representation. In contrast to the adiabatic states $|j\rangle$ diabatic states $|j^d\rangle$ are not uniquely defined. They can be obtained from the adiabatic-diabatic unitary transformation or specified in quantum chemical calculations. The convenient for the nuclear dynamical treatment choice of the diabatic basis is such when the single derivative $(\partial/\partial R)$ matrix elements disappear at any R. In this case the coupled channel equations have the form

$$\left[-\frac{\hbar^2}{2M}\frac{d^2}{dR^2} + H_{jj} + \frac{\hbar^2}{2M}\frac{J(J+1)}{R^2} - E_{tot}\right]F_j^d(R) = -\sum_{k\neq j} H_{jk}F_k^d(R), \qquad (4)$$

where $H_{jk} = \langle j^d|H_e|k^d\rangle$ are the matrix elements of the electronic Hamiltonian H_e in the diabatic representation. In general, the coupled channel equations in a diabatic representation have also the single and double derivative matrix elements in addition to the off-diagonal Hamiltonian matrix elements.

The program used in the present work for numerical integration of the coupled channel equations (2) with the proper boundary conditions is described in reference [9]. The procedure for extracting the nonadiabatic $i \to f$ transition probabilities P_{if} from the solution of the coupled channel equations via the outgoing amplitudes or via the scattering matrix elements is described in references [9,10,26,27]. Then the inelastic cross sections are computed as a sum over the total angular momentum quantum number J

$$\sigma_{if}(E) = \frac{\pi\hbar^2 p_i^{stat}}{2\,M\,E}\sum_J P_{if}(J,E)\,(2J+1), \qquad (5)$$

where p_i^{stat} is the statistical probability for population of the initial channel i and M is the reduced mass of the collided partners. For both systems under consideration $p_i^{stat} = 1/4$ because only the singlet molecular states are treated. Except for very low energies, a large number of J values contribute to the cross section, giving J the character of a quasicontinuous variable. In this case J can be replaced by the impact parameter b

$$b = \hbar \sqrt{\frac{J(J+1)}{2ME}}, \tag{6}$$

and the inelastic cross section can be computed as the integral over b

$$\sigma_{if}(E) = 2\pi p_i^{stat} \int_0^\infty P_{if}(b,E)\, b\, db. \tag{7}$$

In the present work the coupled channel equations (2) are solved in the two-channel approximation.

2.2 Perturbation

An additional check of the numerical calculations of the nonadiabatic transition probabilities and the inelastic cross sections can be performed based on a perturbation theory approach. If a system traverses the nonadiabatic regions mainly adiabatically, which is the result of the small nonadiabatic couplings, the two-state coupled channel equations (2) can be solved by means of the perturbation theory approach [28]. Assume that in the asymptotic $R \to \infty$ region the incoming current entirely populates the initial i channel and that the nonadiabatic couplings (both the single and the double derivative matrix elements) are weak, which means that F_f is small together with F_f', and the right hand side of the corresponding equation for F_i is negligible. In a first approximation the radial wave function F_i can be found as a solution of the corresponding homogeneous differential equation:

$$F_i \approx F_i^{el}, \tag{8}$$

where F_i^{el} is a solution of the equation

$$\left[-\frac{\hbar^2}{2M}\frac{d^2}{dR^2} + V_i(R) + \frac{\hbar^2}{2M}\frac{J(J+1)}{R^2} - E_{tot}\right] F_i^{el}(R) = 0 \tag{9}$$

with the proper scattering boundary conditions:

$$F_i^{el} \to 0 \quad \text{as} \quad R \to 0 \tag{10}$$

and

$$F_i^{el} \to \frac{1}{\sqrt{k_i}} \left[e^{-i(k_i R+\delta)} + e^{+i(k_i R+\delta)}\right] \quad \text{as} \quad R \to \infty, \tag{11}$$

where k_i is the channel wave number in the asymptotic region

$$k_i = \frac{\sqrt{2M[E_{tot} - V_i(\infty)]}}{\hbar}. \tag{12}$$

Then assuming the equation (3) valid, we find that the radial wave function F_f in the final channel in the asymptotic region is proportional to the usual outgoing wave function $F_f^{(+)} = \exp(+i(k_f R + \delta'))/\sqrt{k_f}$

$$F_f = A\, F_f^{(+)}, \tag{13}$$

where the amplitude A is equal to

$$A = \frac{1}{2}\int_0^\infty \langle i|\frac{\partial}{\partial R}|f\rangle \left[F_i^{el}\frac{dF_f^{el}}{dR} - F_f^{el}\frac{dF_i^{el}}{dR}\right] dR, \tag{14}$$

and F_f^{el}, the elastic scattering wave function in the final channel f, is the solution of the equation similar to (9) with the subscript f instead of i.

Finally, the nonadiabatic transition probability P_{if} within the perturbation approach is given by

$$P_{if} = \frac{1}{4}\left|\int_0^\infty \langle i|\frac{\partial}{\partial R}|f\rangle \left[F_i^{el}\frac{dF_f^{el}}{dR} - F_f^{el}\frac{dF_i^{el}}{dR}\right] dR\right|^2. \tag{15}$$

If the nonadiabatic coupling goes to zero in the asymptotic ($R \to \infty$) region, which is often the case in practical applications, see, e.g., equation (19) below, then the integral (14) converges and the formula (15) gives a well defined transition probability.

Often the radial nonadiabatic couplings go to constant nonvanishing values at $R \to \infty$, see, e.g., references [26,27] and references therein. The problem is known as electron translation. In this case the integral (14) does not converge, and hence the transition probability (15) indicates an oscillatory behaviour as a function of the upper integration limit. This is exactly what the accurate quantum dynamical calculations provide [26,27]. In such situation special care should be taken in order to extract a transition probability [26,27]. In the two-channel case this probability can be calculated by averaging the results of equation (15) over a period of oscillations.

2.3 The Landau-Zener model

The Landau-Zener model is usually formulated as the two-state problem in the diabatic basis, equations (4), with constant off-diagonal matrix elements $H_{if} = H_{fi}$ and linear R-dependent diagonal matrix elements H_{ii} and H_{ff} [13,21]. The LZ model requirements should be fulfilled at least within a nonadiabatic region. The nonadiabatic $i \to f$ transition probabilities after a double traverse of the nonadiabatic region and an averaging over the rapidly oscillating Stückelberg phase reads

$$P_{if}(v) = 2\, p_{if}(v)\,[1 - p_{if}(v)], \tag{16}$$

where v is the radial velocity of the colliding atoms at the center of the nonadiabatic region R_c, the crossing of the diabatic potentials, and $p_{if}(v)$ is the nonadiabatic transition probability after a single traverse of the nonadiabatic region [13,21]:

$$p_{if}(v) = \exp\left(-\xi/v\right), \tag{17}$$

ξ being a parameter of the model. In the diabatic representation the LZ parameter is

$$\xi = \xi_{di} = 2\pi H_{if}^2/\hbar|H'_{ii} - H'_{ff}|, \tag{18}$$

where primed quantities refer to derivatives with respect to R. All values are evaluated at R_c.

Quantum chemical data are more often obtained in an adiabatic representation rather than in a diabatic one. Knowing the 2×2 Hamiltonian matrix in a diabatic representation, it is easy to calculate adiabatic potentials and a radial nonadiabatic coupling $\langle i|\partial/\partial R|f\rangle$. Assuming that the diabatic basis functions are independent of the internuclear separation one gets the radial nonadiabatic coupling in the Lorentzian form:

$$\left\langle i \left| \frac{\partial}{\partial R} \right| f \right\rangle = \frac{\tau}{(R - R_c)^2 + 4\tau^2}, \tag{19}$$

where $\tau = H_{if}/|H'_{ii} - H'_{ff}|$. The integral of the nonadiabatic coupling (19) over R is equal to $\pi/2$, which gives a useful test of applicability of the LZ model. At $R = R_c$ the absolute value of the nonadiabatic coupling matrix element has a maximum $D = \max|\langle i|\partial/\partial R|f\rangle|$ and the splitting of adiabatic potential energies has a minimum ΔV. Finally, one can readily find the relations between the diabatic and the adiabatic characteristics of the model at R_c:

$$H_{if} = \Delta V/2, \tag{20}$$

$$|H'_{ii} - H'_{ff}| = 2\,D\,\Delta V. \tag{21}$$

Substituting equations (20, 21) into the equation (18), one gets the LZ parameter in the adiabatic representation:

$$\xi = \xi_{ad} = \pi\Delta V/4\hbar D. \tag{22}$$

Thus, within the two-state Landau-Zener model the nonadiabatic transition probability can be evaluated by means of equations (16, 17) where the LZ parameter is calculated either in the diabatic representation by equation (18) or in the adiabatic representation by equation (22). In the exact Landau-Zener case the results of using different representations coincide.

3 Results and discussions

3.1 H + Na collisions

Consider first the H + Na collisions. The quantum chemical data for the NaH system are discussed in references [9,29–33] and references therein. Both the adiabatic and diabatic potential energies have been calculated. The radial nonadiabatic couplings have been computed by means of the pseudopotential approach [30] and directly [9] by means of the ab initio multireference single- and double-excitation configuration interaction (MRD-CI) method [34,35]. The results of these calculations agree reasonably with each other.

The most important nonadiabatic region for the excitation process takes place between the $X^1\Sigma^+$ and $A^1\Sigma^+$ molecular states around $R \approx 7.5$ a.u., where the adiabatic potentials are approaching each other and the coupling has the maximum. As shown below, at low collision energies the inelastic cross section is sensitive to the fine details of the radial coupling. For this reason in the present work the new calculations of the $X^1\Sigma^+$ and $A^1\Sigma^+$ adiabatic potentials and the single derivative radial coupling between these states are performed in the framework of MOLPRO [36]. The correlation-consistent polarized valence-quadruple zeta (cc-pVQZ) basis set for H atom and the augmented cc-pVTZ basis set for Na atom have been employed. Using this basis set, a state-averaged (over the states treated) full-valence complete-active space self-consistent field (CASSCF) was performed followed by a multi-reference configuration interaction (MRCI) calculation. The calculated MRCI potentials agree well with those of reference [9] shown in Figures 1 and 2 of that paper. The MRCI radial coupling calculated in the present work is shown in Figure 1 of the present paper by circles. It is seen that it generally agrees with the MRD-CI coupling [9] (the solid curve). The main deviation is in the region of the maximum around $R \approx 7.5$ a.u.: the MRCI coupling has the maximum of $D = 0.181$ a.u. at $R_c = 7.45$ a.u. versus the MRD-CI value of 0.148 a.u. at 7.35 a.u. [9], that is, 20% larger. Both MRD-CI and MRCI calculations show that there are 2 broad overlapping nonadiabatic regions between the $X^1\Sigma^+$ and $A^1\Sigma^+$ states: around $R \approx 7.5$ a.u. and around $R \approx 1.6$ a.u. of opposite signs. This results in remarkable deviation of the calculated couplings from the Lorentzian form (19) used in the LZ model with the parameters obtained below in the diabatic representation (see the dashed line in Fig. 1). In particular, the maximum of the Lorentzian form is 40-70% larger than the maxima of the calculated couplings. Moreover, the corresponding integral of a CI nonadiabatic

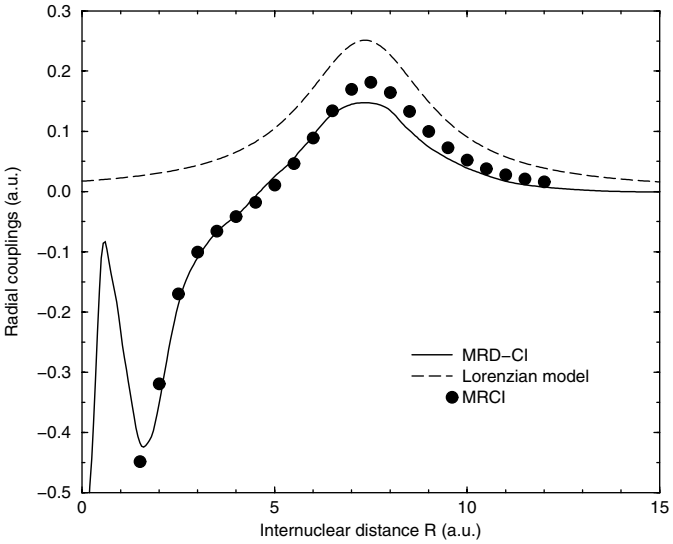

Fig. 1. The nonadiabatic radial coupling between the $X^1\Sigma^+$ and $A^1\Sigma^+$ states of the NaH quasimolecule. The circles are the MRCI calculations, the solid curve is the MRD-CI coupling [9], the dashed line is the Lorentzian model (19).

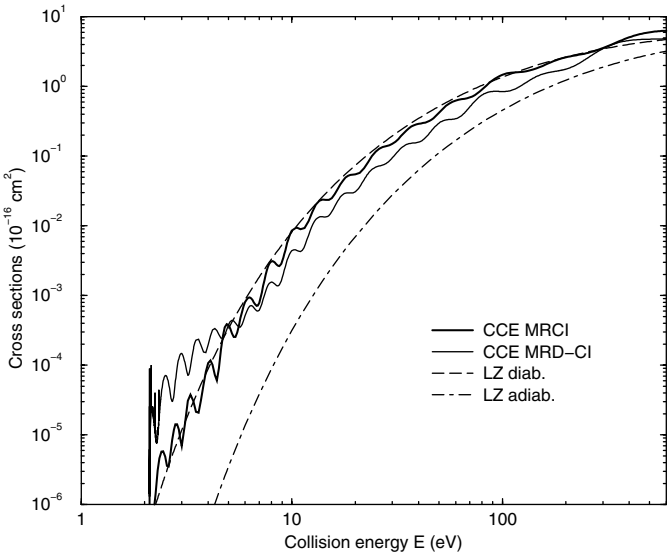

Fig. 2. The energy dependence of the Na($3s \rightarrow 3p$) excitation cross sections in collisions with the hydrogen atoms. The thick solid curve is the full quantum calculation [the solution of the coupled channel Eqs. (2)] with the MRCI nonadiabatic coupling calculated in the present work. The thin solid curve is the quantum cross section with the MRD-CI coupling [9]. The dashed and the dot-dashed lines are the LZ model cross sections in the diabatic and the adiabatic representations, respectively.

coupling over the nonadiabatic region around $R \approx 7.5$ a.u. is about $\pi/4$, that is, nearly twice smaller than $\pi/2$ obtained from the Lorentzian form (19).

The adiabatic splitting at the center of the nonadiabatic region is $\Delta V = 0.0436$ a.u. This leads to the LZ parameter $\xi_{ad} = 0.189$ a.u. The diabatic potentials reconstructed from the adiabatic ones intersect each other at $R_c = 7.6$ a.u. and provide $H_{if} = 0.0209$ a.u. and $|H'_{ii} - H'_{ff}| = 0.021$ a.u. This gives the LZ parameter $\xi_{di} = 0.130$ a.u. This value is in good agreement with the parameter $\xi_{di} = 0.129$ a.u. of reference [8]. Reference [32] displays the diabatic NaH potentials and gives $R_c = 7.83$ a.u. and $\Delta V = 0.0441$ a.u., but does not give $|H'_{ii} - H'_{ff}|$, which does not allow us to calculate ξ_{di}. The estimation gives $\xi_{di} \approx 0.10$ a.u. which is close to the value used in the present paper. For the NaH system ξ_{ad} is nearly 50% larger than ξ_{di}, which leads to much smaller transition probabilities and smaller cross sections in the adiabatic representation than in the diabatic one. The point is that the Landau-Zener model assumptions are not completely fulfilled and, hence, the equation (21) is not fulfilled. It should be emphasized that ξ_{ad} is obtained directly from the quantum chemical calculations, while ξ_{di} is extracted by the usual procedure: from the reconstruction of the diabatic potentials from the adiabatic ones, not from the adiabatic-diabatic transformation.

In the present work the Na($3s \rightarrow 3p$) + H excitation cross sections are calculated within the rigorous two-state quantum dynamical treatment with the new (MRCI) and the old (MRD-CI [9]) quantum chemical data, as well as within the LZ model in both the diabatic and the adiabatic representations. As the MRCI adiabatic potentials practically do not deviate from the MRD-CI ones, the latter are employed in both quantum dynamical calculations in order to show the influence of the radial coupling on the inelastic cross section. The calculated cross sections from the energy threshold till 600 eV are shown in Figure 2. It is seen that at $E > 5$ eV the quantal cross sections with the MRD-CI and the MRCI couplings are close to each other except for the Stückelberg oscillations; the MRCI cross section is slightly larger the MRD-CI one, which is the result of the larger MRCI coupling in the nonadiabatic region around $R \approx 7.5$ a.u. At $E < 5$ eV the relation is inverse: the MRD-CI cross section is larger than the MRCI one up to a factor of 20 in the energy threshold region. This fact is studied in details below. The narrow peaks of the cross section just above the energy threshold are the results of the orbital resonances.

The rigorous quantal cross sections can be compared with ones obtained within the Landau-Zener model, which are also depicted in Figure 2. The quantal cross sections show the oscillatory behaviour, which is the result of the Stückelberg oscillations. The model calculations do not have such oscillations as the transition probabilities (16) are averaged over the Stückelberg phases. There is a large difference, up to 5 orders of magnitude, in the LZ cross sections computed in the different representations, especially at low collision energies. At high energies the difference is smaller, down to a factor of 2 at $E = 600$ eV. At the collision energies under consideration the system traverses the nonadiabatic region nearly adiabatically, and hence the LZ model cross section in the diabatic representation is greater than in the adiabatic one because $\xi_{ad} > \xi_{di}$. The discrepancy between the LZ model cross sections in different representations is based on the fact that the LZ model requirements are not fulfilled in the case treated.

The LZ model cross section in the diabatic representation agrees with the MRCI quantal result especially for collision energies $E > 10$ eV. The energy dependence of the MRD-CI cross section indicates a Landau-Zener-like behaviour (an approximate proportionality between the rigorous and the model cross sections besides the Stückelberg oscillations) at $E > 10$ eV. At $E < 10$ eV the rigorous cross section shows the non-Landau-Zener-like behaviour. The origin of the non-Landau-Zener-like behaviour of the cross sections is discussed below.

The finding that the small variation in the nonadiabatic coupling leads to large deviation in the cross section at low energies is interesting and needs an explanation. For this reason the numerical solutions of the coupled channel equations (2) are checked by the analytic formula (15) obtained within the perturbation approach. The results of this check are shown in Figures 3, 4 and 5, where the Na($3s \rightarrow 3p$) + H transition probabilities multiplied by the impact parameter [that is, the integrand of the cross section (7)] are depicted as a function of the impact parameter at $E = 10$, 5 and 3 eV, respectively. It is seen from these figures that the transition probabilities obtained by means of the perturbation

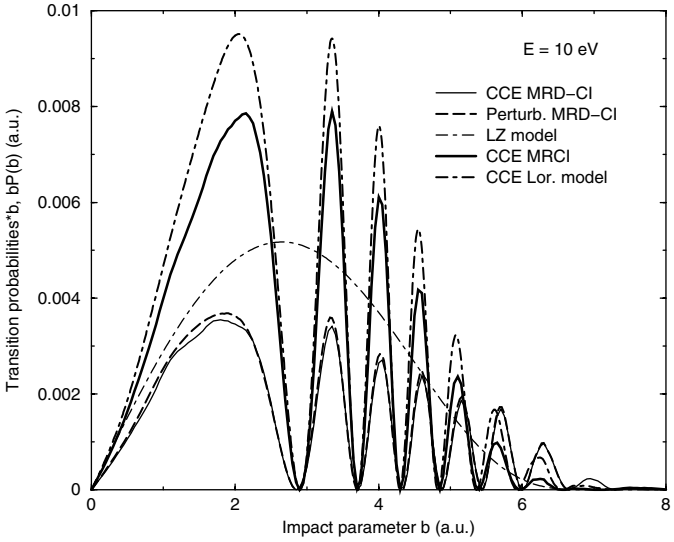

Fig. 3. The Na($3s \rightarrow 3p$) + H transition probabilities multiplied by the impact parameter b as a function of the impact parameter at $E = 10$ eV. The thin solid line is the solution of CCE (2) with the MRD-CI coupling [9]; the dashed line is the result of the perturbation formula (15) with the same coupling; the thick solid line is the solution of CCE (2) with the MRCI coupling; the thin dot-dashed line is the Landau-Zener model in the diabatic representation; the thick dot-dashed line is the solution of CCE with the Lorentzian coupling.

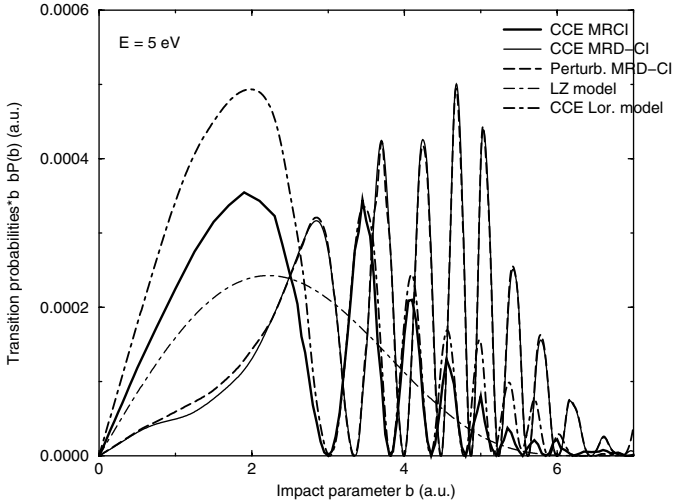

Fig. 4. The Na($3s \rightarrow 3p$) + H transition probabilities multiplied by the impact parameter as a function of the impact parameter at $E = 5$ eV. The notations are the same as in Figure 3.

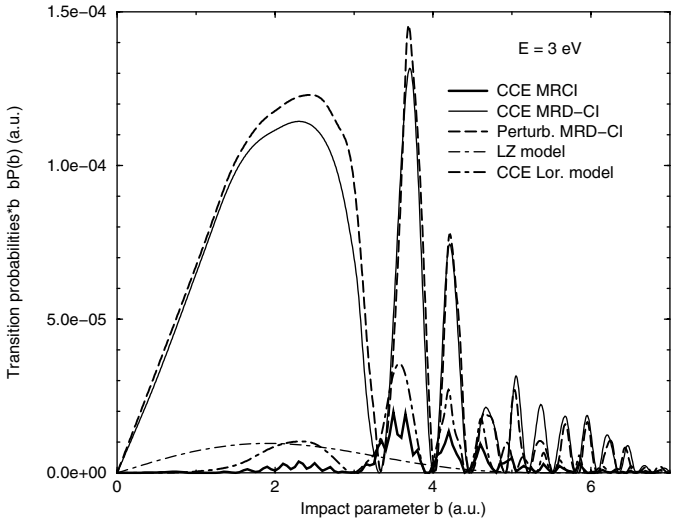

Fig. 5. The Na($3s \rightarrow 3p$) + H transition probabilities multiplied by the impact parameter as a function of the impact parameter at $E = 3$ eV. The notations are the same as in Figure 3.

formula agree well (typically within 1%) with the solutions of the coupled channel equations. The discrepancy does not exceed 10% at some impact parameters and at very low collision energies where the transition probabilities are small (10^{-6}–10^{-4}). This result holds also with using of the MRCI coupling (not shown in the figures). This allows us to make the conclusion that the quantal results are accurate.

Figure 3 shows that at relatively high collision energies practically the same range of the impact parameter determines the cross sections calculated by different means. The Stückelberg oscillations are clearly seen in the solutions of CCE with all couplings. The Landau-Zener result agrees well with the averaged solution of CCE with the Lorentzian coupling. It is also seen that at high energies increasing of the radial coupling in the nonadiabatic region around $R \approx 7.5$ a.u. (Fig. 1) increases the transition probabilities and, hence, the cross section. This result is understandable from the perturbation formula (15), although it should be pointed out that there is no exact proportionality between the three couplings treated in the present case. Note the MRCI transition probabilities are nearly two times greater than the MRD-CI ones.

Decreasing the collision energy changes the situation. At $E = 5$ eV (Fig. 4) the MRD-CI transition probabilities have the same values of magnitude as the MRCI probabilities and even larger at large impact parameters ($b \approx 3$–6 a.u.). This results in practically equal cross sections, see Figure 2. Further decreasing the energy, e.g., $E = 3$ eV, Figure 5, leads to the much larger (an order of magnitude) MRD-CI probabilities than both the MRCI and LZ ones. Moreover, considerable contribution in the quantal cross sections comes from a large impact parameter region where the LZ probabilities are zero, the so-called grazing incidence. This results in a non-Landau-Zener-like behaviour of the energy dependence of the quantum cross sections at low energies, see Figure 2. There are two reasons for this. First, the MRCI and MRD-CI couplings indicate two overlapping nonadiabatic regions, see Figure 1, which leads to the Rosenthal oscillations (the interference effect between two nonadiabatic regions). The analyses of the transition probabilities calculated by means of the perturbation formula (15) show that the integrands are oscillating functions, so are the amplitudes (14) as a function $A(R_{end})$ of the upper integration limit R_{end} with large

amplitudes of oscillations. If a Lorentzian coupling (19) is used, then the final amplitude $A(R_{end} \to \infty)$ is much smaller than the maximum of $A(R_{end})$ at an intermediate R_{end}. When a radial coupling changes a sign (both the MRCI and the MRD-CI couplings), the Rosenthal oscillations could provide the final amplitude $A(R_{end} \to \infty)$ much smaller or much greater (or any value in between) then the amplitude A with the Lorentzian coupling. For example, at $E = 10$ eV the Rosenthal oscillation leads to the MRD-CI transition probabilities twice smaller than the MRCI ones (Fig. 3), while at $E = 3$ eV the MRD-CI probabilities are by an order of magnitude greater than the MRCI ones (Fig. 5). In other words, the oscillations of the $A(R_{end})$ amplitude with the MRD-CI coupling are cut-off by changing of sign of the coupling in such a way that these oscillations are left uncompensated leading to a large final amplitude $A(R_{end} \to \infty)$.

The second reason is in the grazing incidence. At low collision energies and large impact parameters the classical turning points are close to or even inside the nonadiabatic region. In this case the standard LZ formula (17) is not valid, as this formula was obtained under the assumption that classical turning points are far from a nonadiabatic region. When classical turning points are close to a nonadiabatic region, the formula for a nonadiabatic transition has corrections [21,24,37,38] compared with the standard LZ expression. It is seen from Figure 5 that at grazing incidence the LZ model underestimates the transition probabilities as compared with the solutions of CCE with all radial couplings (the MRCI, MRD-CI and Lorentzian ones). The cut-off in the LZ model is determined by the positive radial energy with respect to the mean potential energy at the center of a nonadiabatic region, while quantum transitions could occur even in the classically forbidden regions where wave functions are still nonzero. This explains the influence of the grazing incidence.

Thus, at low collision energies the quantal transition probabilities and cross sections are very sensitive to the nonadiabatic coupling. This is not the result of numerics. In the case treated this is the result of the Rosenthal oscillations.

3.2 H + Li collisions

Consider now the H + Li collisions. The quantum chemical data (the potential energies and the nonadiabatic couplings) are discussed in detail in references [10,39–42]. Both the diabatic and adiabatic potentials have been calculated. The radial nonadiabatic couplings have been computed by numerical differentiation of the configuration interaction coefficients [10] [see Fig. 1 of that paper]. It was shown that most important for the excitation process is the nonadiabatic region between the $X\ ^1\Sigma^+$ and $A\ ^1\Sigma^+$ molecular states around $R \approx 7$ a.u. The diabatic potentials cross each other, the adiabatic potentials undergo an avoided crossing, the nonadiabatic coupling has a form close to Lorentzian (although not exactly), and the area under the coupling peak is close to $\pi/2$. Thus the Landau-Zener model is expected to be appropriate,

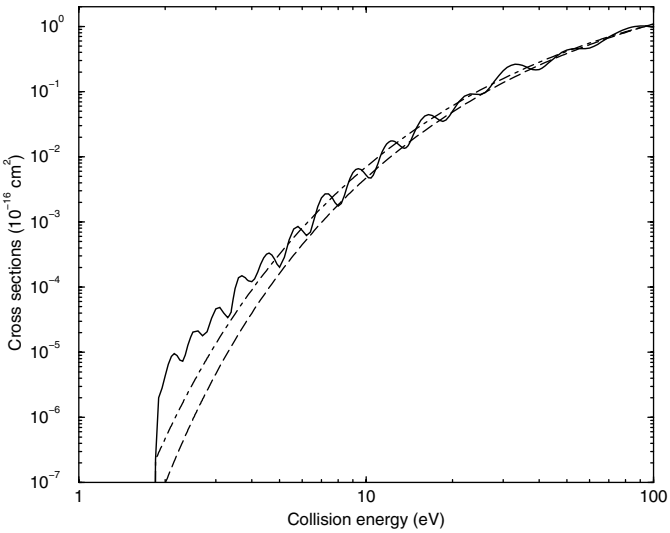

Fig. 6. The energy dependence of the Li($2s \to 2p$) excitation cross sections in collisions with the hydrogen atoms. The solid line is the full quantum calculation for the LiH($^1\Sigma^+$) quasimolecule. The dashed and the dot-dashed lines are the cross sections from the Landau-Zener model in the diabatic and the adiabatic representations, respectively.

despite the inexact linear dependence of the diabatic potentials and the varying off-diagonal matrix elements.

In the diabatic representation the LiH Landau-Zener parameter is $\xi_{di} = 0.145$ a.u. at $R_c = 7.3$ a.u. ($H_{if} = 0.022$ a.u., $|H'_{ii} - H'_{ff}| = 0.021$ a.u.). In the adiabatic representation, when the center of the nonadiabatic region is defined as the maximum of the nonadiabatic coupling, the LZ parameter ξ_{ad} is equal to 0.135 a.u. at $R_c = 6.75$ a.u. ($\Delta V = 0.0455$ a.u., $D = 0.264$ a.u.). Besides the small difference in R_c in the adiabatic and the diabatic representations, the deviation of the LZ parameters in different representation occurs because equation (21) is not exactly fulfilled, while equation (20) holds approximately. The different LZ parameters lead to some deviation in cross sections.

In the present work the quantum cross section is calculated by integrating of the two-state coupled channel equations (2) for the low-energy H + Li collisions (up to $E = 100$ eV). The result is shown in Figure 6 by the solid line and compared with the Landau-Zener cross sections calculated in both the diabatic and the adiabatic representations (the dashed and the dot-dashed lines). At collision energies $E > 40$ eV the LZ cross sections in the different representations practically coincide, while at lower energies there is a difference up to a factor of 5. At the collision energies under consideration the system traverses the nonadiabatic region nearly adiabatically, which results in the larger cross section in the adiabatic representation as $\xi_{ad} < \xi_{di}$ [see Eq. (17)]. Note the inverse relation for H + Na collisions. The LZ cross section calculated in the adiabatic representation agrees better with the rigorous quantum calculation than the cross section computed in the diabatic basis. The quantal cross section (Fig. 6) shows the oscillatory behaviour, which is the result of the

Stückelberg oscillations. The model calculations do not have such oscillations. The orbital resonances are omitted in the H + Li cross section calculation. Besides the oscillations the quantal cross section displays the LZ behaviour at the collision energies $E > 5$ eV. At $E < 5$ eV the quantal cross section deviates from the model calculation up to an order of magnitude indicating a non-Landau-Zener-like behaviour of the cross section. The reasons for the deviation are the same as for Na + H collisions: (i) the calculated radial coupling differs from the Lorentzian form and (ii) the grazing incidence affects the low-energy cross section. The magnitude of the transition probabilities at grazing incidence is rather small, around 10^{-4}, and when the transition probabilities at smaller impact parameters have much larger values, the contribution from the grazing incidence is negligible. That is why this effect is significant at the collision energies just above the energy threshold.

4 Conclusions

In the present work the cross sections for the Li($2s \rightarrow 2p$) and Na($3s \rightarrow 3p$) electronic excitation by H atom impact for energies between the thresholds and 100 eV or 600 eV, respectively, are calculated by means of the full quantum approach in the two-state approximation, as well as by means of the standard two-state Landau-Zener model in both the diabatic and the adiabatic representations. The new calculations of the $X\ ^1\Sigma^+$ and $A\ ^1\Sigma^+$ potentials and the nonadiabatic radial coupling are performed by means of the MRCI method for the NaH molecule. These new data, as well as ones from the previous calculations [9, 10] (for both NaH and LiH) are employed in the dynamical treatment. The results of the numerical integration of the coupled channel equations are checked by independent calculation of nonadiabatic transitions by means of a simple analytic formula. The formula is derived within the framework of the perturbation approach. The CCE and the perturbation results agree well with each other indicating that the quantum calculations are accurate.

The Landau-Zener model cross sections are computed for the same transitions in both diabatic and adiabatic representations. It is found that in practical applications of the Landau-Zener model the different representations may give close results (when the Landau-Zener requirements are more or less fulfilled) as in H + Li collisions at relatively high collision energies, but sometimes the results of using the different representations may deviate substantially from each other, up to several orders of magnitude as in the H + Na case. It is found that the adiabatic representation of the Landau-Zener model may agree with the accurate quantum dynamical calculations better than does the diabatic representation (H + Li collisions), and sometimes the diabatic representation works better than the adiabatic one (H + Na collisions).

It is shown that at low collision energies the quantum inelastic transition probabilities and cross sections are very sensitive to the nonadiabatic coupling. The origin of this sensitivity is in the Rosenthal oscillations between two overlapping nonadiabatic regions. This effect together with the grazing incidence lead to a non-Landau-Zener-like behaviour of inelastic cross sections at low energies (a few eV above the energy thresholds). At high collision energies the accurate quantal inelastic cross sections indicate a Landau-Zener-like behaviour besides the Stückelberg oscillations. Thus, the same nonadiabatic region can provide both Landau-Zener-like and non-Landau-Zener-like behaviour of the cross section depending on the collision energy range.

The author is indebted to Prof. J. Grosser for fruitful discussions and thankful to Dr. S. Mishra for his help in performing MOLPRO calculations. This work was partially supported by INTAS (the project No. 03-51-6170) and by the Swedish Royal Academy of Sciences.

References

1. D. Lambert, Phys. Scr. **T47**, 186 (1993)
2. H. Holweger, Phys. Scr. **T65**, 151 (1996)
3. M.F. Mott, H.S.W. Massey, *The Theory of Atomic Collisions* (Clarendon, Oxford, 1949)
4. A. Macias, A. Riera, Phys. Rep. **90**, 299 (1982)
5. W. Steenbock, H. Holweger, Astron. Astrophys. **130**, 319 (1984)
6. P.S. Barklem, A.K. Belyaev, M. Asplund, Astron. Astrophys. **409**, L1 (2003)
7. H.W. Drawin, Z. Phys. **211**, 404 (1968)
8. I. Fleck, J. Grosser, A. Schnecke, W. Steen, H. Voigt, J. Phys. B **24**, 4017 (1991)
9. A.K. Belyaev, J. Grosser, J. Hahne, T. Menzel, Phys. Rev. A **60**, 2151 (1999)
10. A.K. Belyaev, P.S. Barklem, Phys. Rev. A **68**, 062703 (2003)
11. L.D. Landau, Phys. Z. Sowietunion **1**, 88 (1932); L.D. Landau, Phys. Z. Sowietunion **2**, 46 (1932)
12. C. Zener, Proc. Roy. Soc. A **137**, 696 (1932)
13. E.E. Nikitin, in *Atomic, Molecular, Optical Physics Handbook*, edited by G.W.F. Drake (AIP Press, New York, 1996), Chap. 47
14. Yu.N. Demkov, V.I. Osherov, Sov. Phys. JETP **26**, 916 (1968)
15. A. Salop, R.E. Olson, Phys. Rev. A **13**, 1312 (1976)
16. A.K. Belyaev, Phys. Rev. A **48**, 4299 (1993)
17. V.N. Ostrovsky, H. Nakamura, J. Phys. B **30**, 6939 (1997)
18. Yu. N. Demkov, V.N. Ostrovsky, Phys. Rev. A **61**, 032705 (2000)
19. Yu.N. Demkov, Sov. Phys. JETP **18**, 138 (1964)
20. E.E. Nikitin, Opt. Spectrosc. **13**, 431 (1962)
21. E.E. Nikitin, S.Ya. Umansky, *Theory of Slow Atomic Collisions* (Springer, Berlin, 1984)
22. V.N. Ostrovsky, Phys. Rev. A **68**, 012710 (2003)
23. E.C.G. Stückelberg, Helv. Phys. Acta **5**, 369 (1932)
24. M.Ya. Ovchinnikova, Sov. Phys. JETP **37**, 68 (1973)
25. C. Zhu, H. Nakamura, Adv. Chem. Phys. **117**, 127 (2001)
26. J. Grosser, T. Menzel, A.K. Belyaev, Phys. Rev. A **59**, 1309 (1999)
27. A.K. Belyaev, D. Egorova, J. Grosser, T. Menzel, Phys. Rev. A **64**, 052701 (2001)

28. A.K. Belyaev, J. Grosser (unpublished)
29. R.E. Olson, B. Liu, J. Chem. Phys. **73**, 2817 (1980)
30. O. Mo, A. Riera, M. Yanez, Phys. Rev. A **31**, 3977 (1985)
31. O. Mo, A. Riera, J. Phys. B **25**, L101 (1992)
32. A.S. Dickinson, R. Poteau, F.X. Gadéa, J. Phys. B **32**, 5451 (1999)
33. T. Leininger, F.X. Gadéa, A.S. Dickinson, J. Phys. B **33**, 1805 (2000)
34. R.J. Buenker, S.D. Peyerimhoff, W. Butscher, Mol. Phys. **35**, 771 (1978)
35. P.J. Bruna, S.D. Peyerimhoff, Adv. Chem. Phys. **67**, 1 (1987)
36. P.J. Knowles, H.-J. Werner, MOLPRO quantum chemistry package (University of Birmingham, 2006)
37. V.K. Bykhovsky, E.E. Nikitin, M.Ya. Ovchinnikova, Sov. Phys. JETP **20**, 500 (1965)
38. E.E. Nikitin, M.Ya. Ovchinnikova, B. Andresen, A.E. de Vries, Chem. Phys. **14**, 121 (1976)
39. A. Boutalib, F.X. Gadéa, J. Chem. Phys. **97**, 1144 (1992)
40. F.X. Gadéa, A. Boutalib, J. Phys. B **26**, 61 (1993)
41. H. Croft, A.S. Dickinson, F.X. Gadéa, J. Phys. B **32**, 81 (1999)
42. O.J. Bennett, A.S. Dickinson, T. Leininger, F.X. Gadéa, Mon. Not. R. Astron. Soc. **341**, 361 (2003)